Non-helical *Helicobacter pylori* show altered gland colonization and elicit less gastric pathology during chronic infection

Laura E. Martínez[1,2], Valerie P. O'Brien[2], Christina K. Leverich[2], Sue E. Knoblaugh[3], Nina R. Salama[1,2*]

[1]Graduate Program in Pathobiology, Department of Global Health, University of Washington, Seattle, WA, 98195, USA.
[2]Division of Human Biology, Fred Hutchinson Cancer Research Center, Seattle, WA, 98109, USA.
[3]Department of Veterinary Biosciences, The Ohio State University, Columbus, OH, 43210, USA.
[*]Correspondence to: nsalama@fredhutch.org

Supplementary Information:

Table S1. Primers used in this study.

Gene name	*H. pylori* gene annotation	Primer	Sequence
Targeted disruption primers			
csd6	HPG27_477[a] (HP0518)[b]	HPG27_476 Forward	gcgcgctctagAAGGAAGAAAAGAGCTTGC[c]
		HPG27_478 Reverse	GCTGGTAGGCTTTGTAATC
Complementation primers			
csd6 at McGee locus[d]	Δ*csd6*::*cat McGee:csd6 :aphA3* in PMSS1	McGee locus Forward	GAGCGAGAATTCAAAGACAACCCCA
		McGee locus Reverse	GGCGATGGGGCTGGGGCGTGCGTGATAGGC

[a]Gene annotation in the human clinical isolate G27 (1).
[b]Gene annotation in the human clinical isolate 26695 (2).
[c]Gene specific sequences are in uppercase and sequences added for cloning are in lower case.
[d]McGee Locus: The intergenic sequence (204322 – 204784) is located between genes HPG27_186 (204127 – 204321) and HPG27_187 (204785 – 205168) in the *H. pylori* strain G27 (1).

Table S2. Histopathologic scoring for inflammation and hyperplasia in mice chronically infected with *H. pylori* for one and three months.

Score	Inflammation	Hyperplasia	Epithelial defects	Oxyntic atrophy	Metaplasia
0	No inflammation	No hyperplasia	No epithelial defects	No oxyntic atrophy	No metaplasia
1	Mild patchy or multifocal islands	Mild elongation of mucosa	Tattered epithelial surface	Decreased chief cells; parietal cells intact	< 50% replacement of oxyntic mucosa by antralized glands
2	Moderate coalescing infiltrate	Increased surface epithelium 2X normal length	Attenuated epithelial surface	Few or no chief cells; parietal cells intact	>50% replacement of oxyntic mucosa by antralized glands
3	Moderate to severe sheets in mucosa and/or submucosa	Increased surface epithelium 3X normal length	Inapparent surface epithelium	No remaining chief cells; loss of parietal cells	Near complete replacement of glands by antralized mucosa
4	Severe florid inflammation into muscularis	Increased surface epithelium 4X normal length +/- dysplasia	Mucosal erosions of surface epithelium	No chief cells and few or no parietal cells remaining	Total replacement of glands by antralized mucosa

References

1. Baltrus DA, Amieva MR, Covacci A, Lowe TM, Merrell DS, Ottemann KM, Stein M, Salama NR, Guillemin K. 2009. The complete genome sequence of *Helicobacter pylori* strain G27. J Bacteriol 191:447-8.
2. Tomb JF, White O, Kerlavage AR, Clayton RA, Sutton GG, Fleischmann RD, Ketchum KA, Klenk HP, Gill S, Dougherty BA, Nelson K, Quackenbush J, Zhou L, Kirkness EF, Peterson S, Loftus B, Richardson D, Dodson R, Khalak HG, Glodek A, McKenney K, Fitzegerald LM, Lee N, Adams MD, Hickey EK, Berg DE, Gocayne JD, Utterback TR, Peterson JD, Kelley JM, Cotton MD, Weidman JM, Fujii C, Bowman C, Watthey L, Wallin E, Hayes WS, Borodovsky M, Karp PD, Smith HO, Fraser CM, Venter JC. 1997. The complete genome sequence of the gastric pathogen *Helicobacter pylori*. Nature 388:539-47.

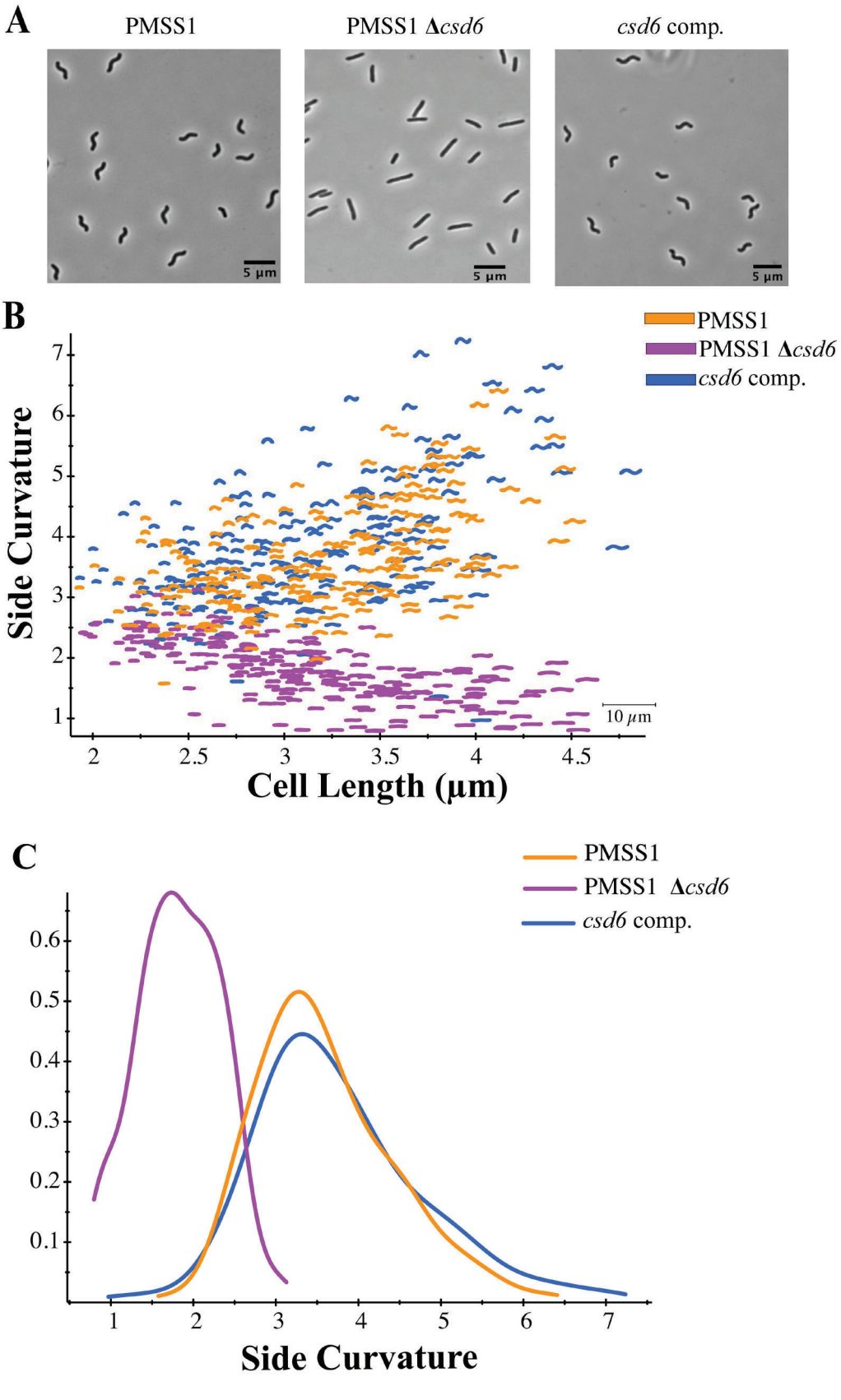
A
PMSS1
PMSS1 Δcsd6
csd6 comp.
5 μm
5 μm
5 μm
B
PMSS1
PMSS1 Δcsd6
csd6 comp.
Side Curvature
Cell Length (μm)
10 μm
C
PMSS1
PMSS1 Δcsd6
csd6 comp.
Side Curvature

Figure S1. Complementation of *csd6* restores helical cell shape. (A) Representative phase contrast images of wild-type PMSS1 bacteria, straight rod (Δ*csd6*), and *csd6* complemented bacteria. Images were acquired at 100 X (oil immersion objective). Scale bar = 5 μm. (B) Side curvature vs. cell length (μm) for individual bacterial cells imaged using phase contrast microscopy of wild-type PMSS1 (orange, n=218), Δ*csd6* (magenta, n=230), and the *csd6* complemented strain (blue, n=212). (C) Smooth histograms summarizing the side curvature distributions acquired for each strain shown in B. No significant difference in side curvature distributions were observed between wild-type and the *csd6* complemented strain ($p = 0.64078$) using Kolmogorov-Smirnov statistics of side curvature distributions. Significant differences in side curvature distributions were observed between wild-type and Δ*csd6*, and between Δ*csd6* and the *csd6* complemented strain, where $p<0.00001$. Data are from two independent experiments.

A.

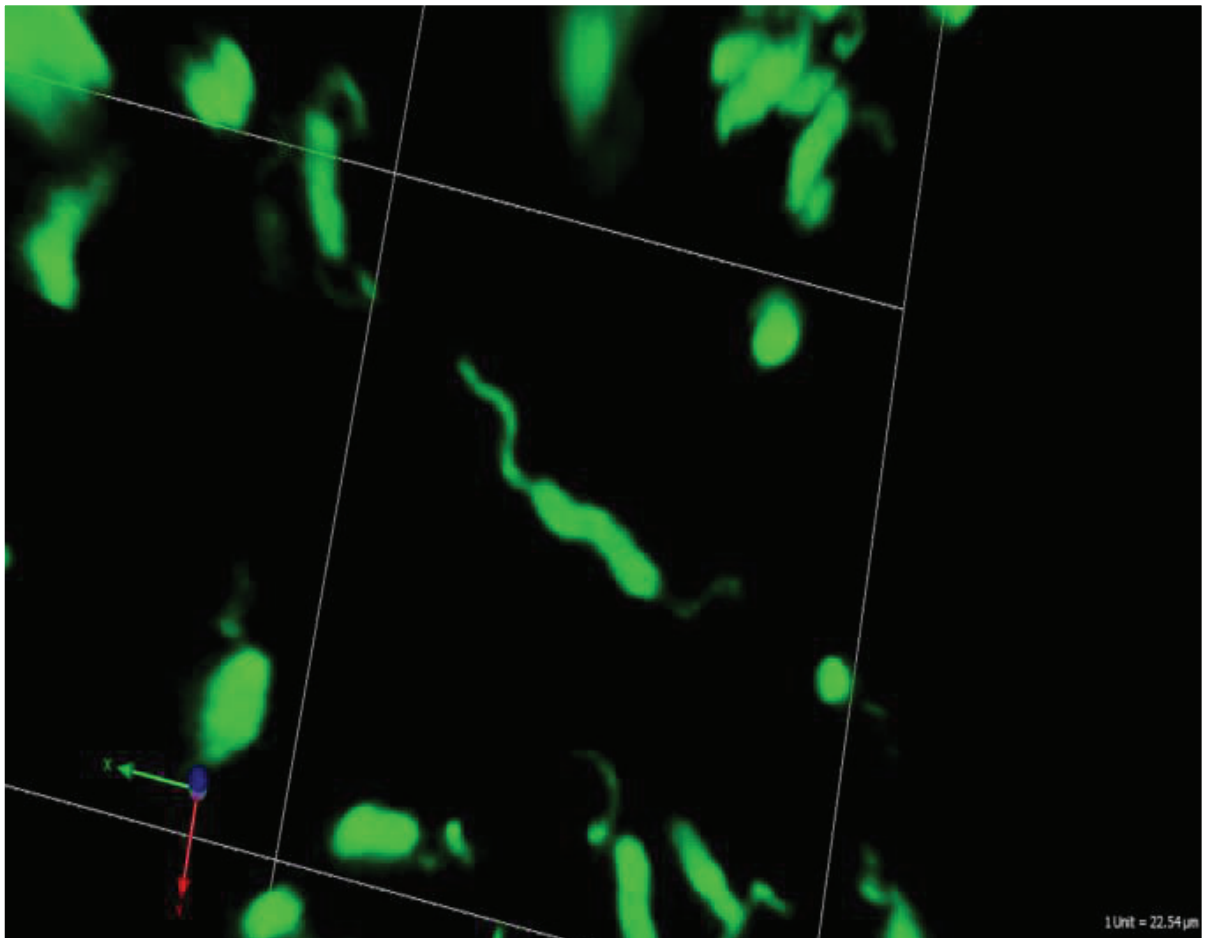

B.

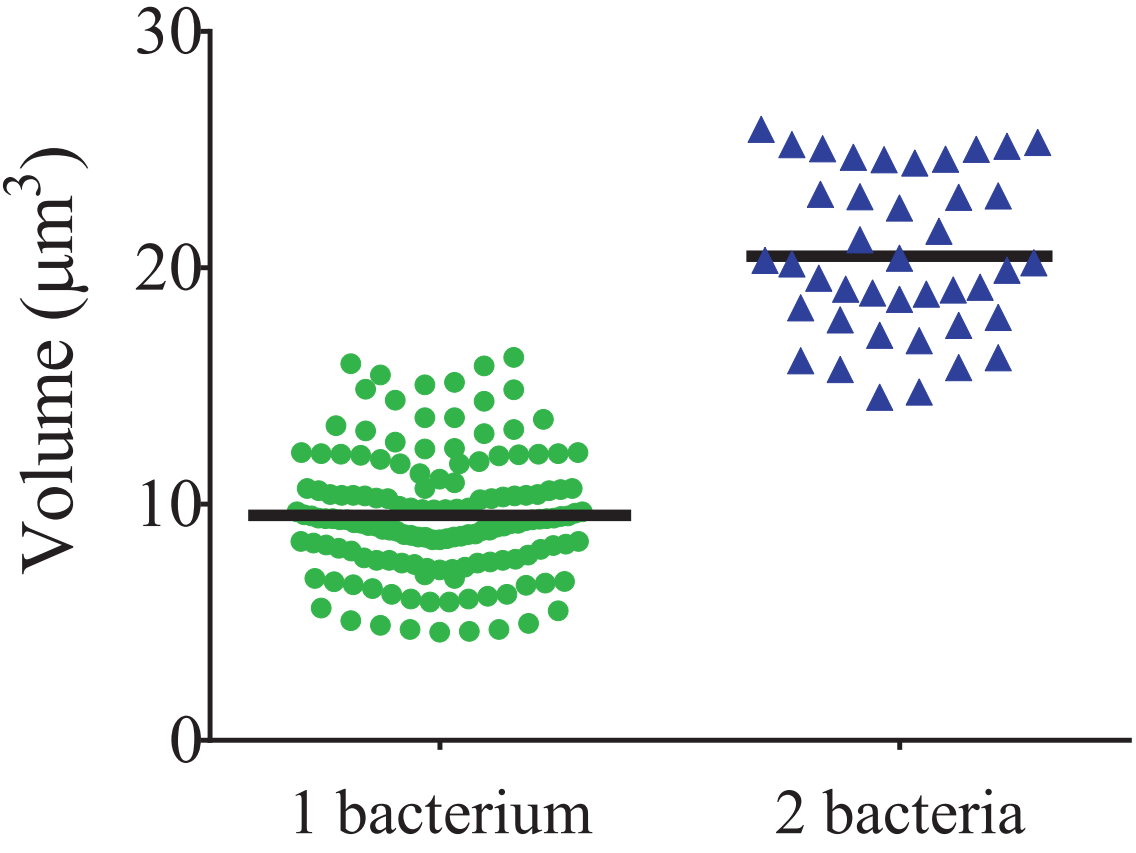

Figure S2. 3D-visualization of *H. pylori* and bacterial quantitation by volumetric image analysis. (A) Representative 3D image of wild-type PMSS1 bacteria (green), which was fixed in 2% PFA, embedded in 4% agarose, and sectioned to generate 200 μm thick sections. 3D-images were generated from Z-stacks collected at 63 X (oil-immersion objective) with a Zeiss LSM 780 confocal microscope. (B) Volumetric image analysis of bacterial cells fixed in 2% PFA (n= 203). Bars indicate the mean. Data are from two independent experiments.

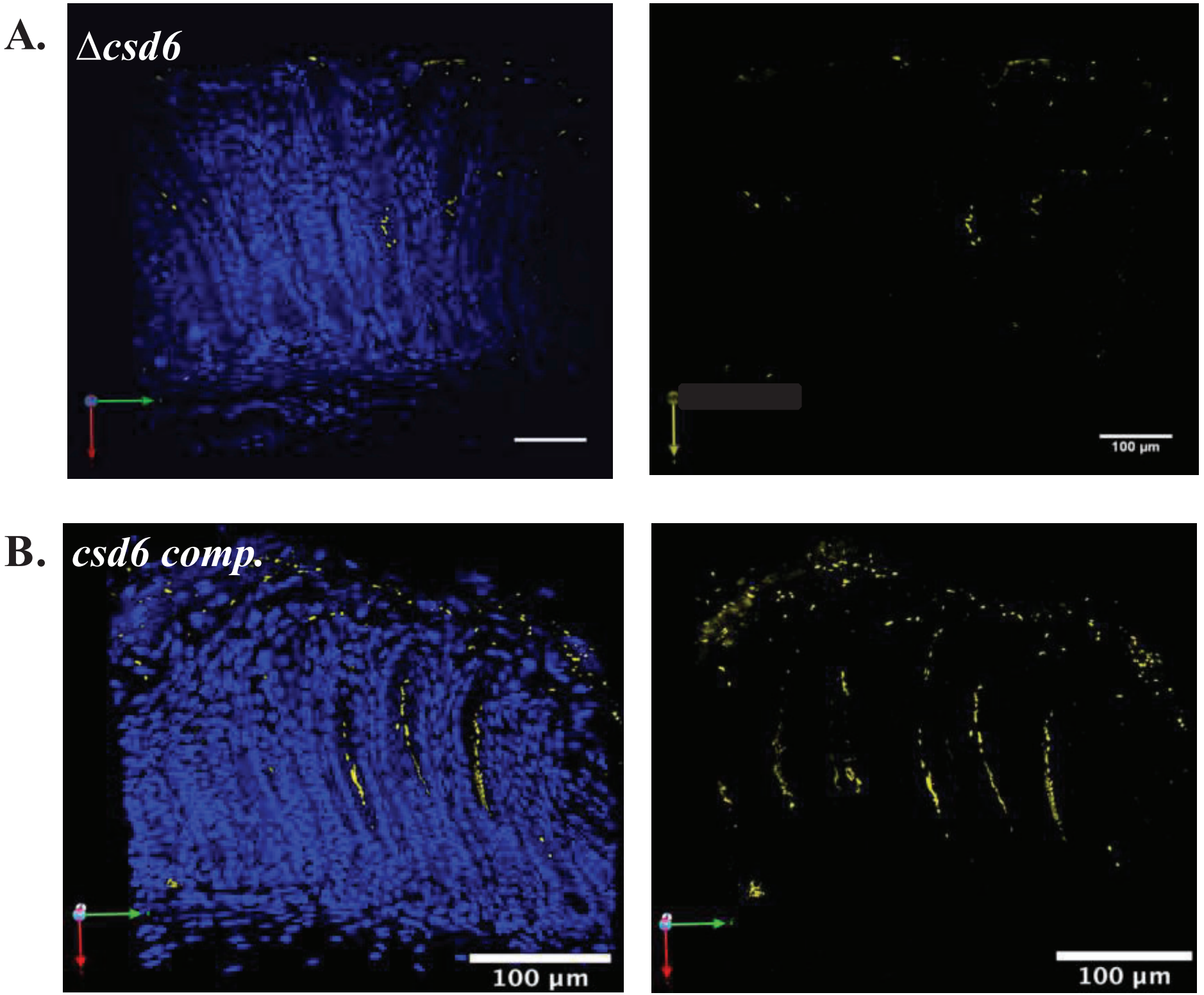
A.
Δcsd6
100 µm
B.
csd6 comp.
100 µm
100 µm

Figure S3. Visualization of bacteria within gastric glands. Thick stomach sections from the one week infections shown in **Figure 2A** were stained for *H. pylori*. Shown are representative images of the antrum of a mouse infected with Δ*csd6* (**A**) or *csd6* complemented (**B**) bacteria**.** Images are maximum intensity projections of Z-stacks, with blue (DAPI, left panel) staining nuclei and yellow staining *H. pylori*. Scale bars = 100 μm. Volumetric analysis for the mouse in **A** is found in **Figure 3C** and **B** is in **Figure 3D**.

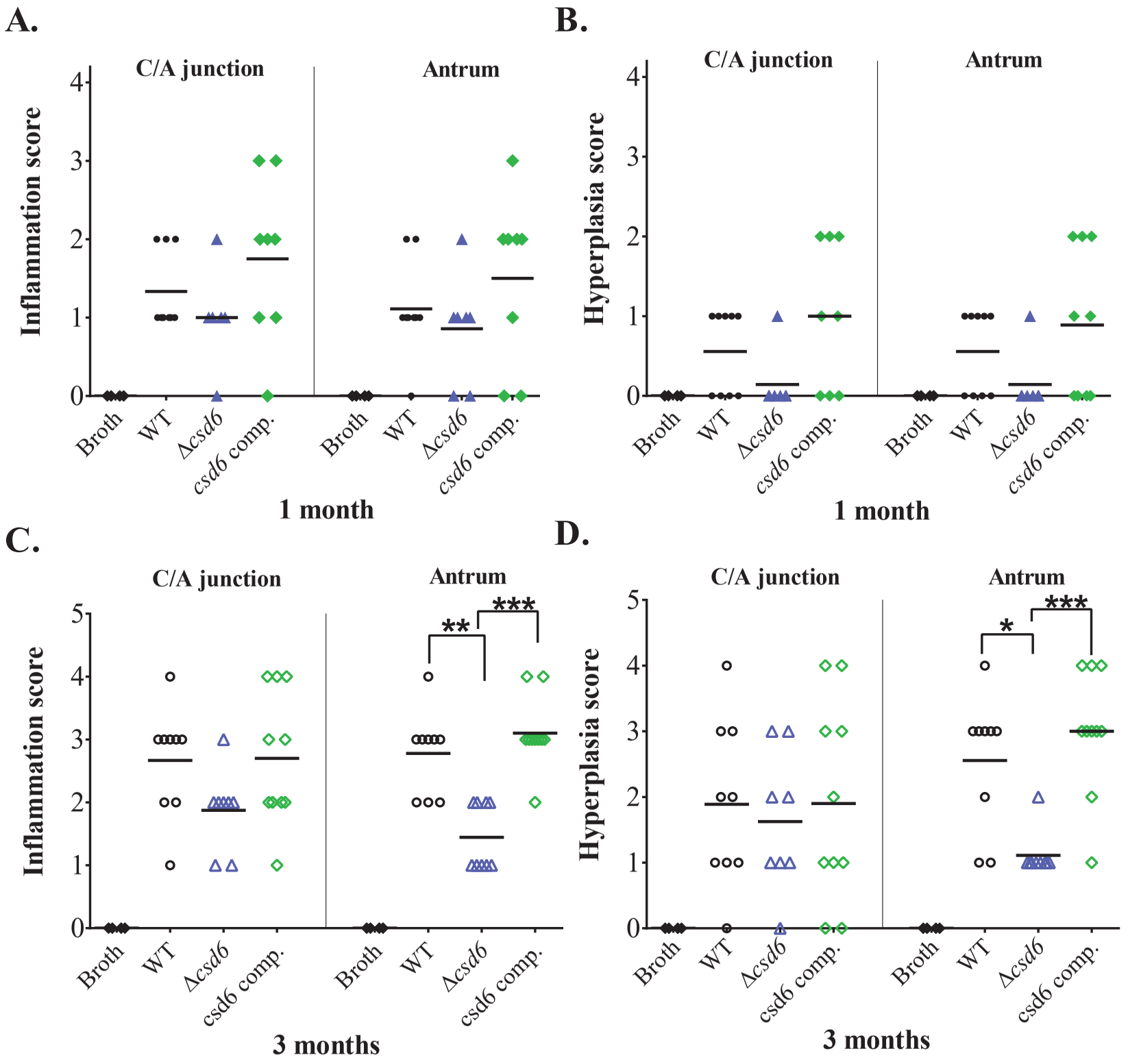
A.
C/A junction
Antrum
Inflammation score
0
1
2
3
4
Broth
WT
Δcsd6
csd6 comp.
1 month
B.
Hyperplasia score
C.
**
***
5
3 months
D.
*

Figure S4. The Δ*csd6* mutant results in decreased inflammation and hyperplasia scores at one and three months of infection. Inflammation (A and C) and hyperplasia (B and D) scores in the corpus/antrum (C/A) junction and antrum at one month (A and B) and three months (C and D) of infection (n=9-11 mice per group). Provided are pathological evaluation scores for all gastric tissue sections analyzed and shown in Fig 5. * $P < 0.05$, ** $P < 0.01$, *** $P < 0.001$, Kruskal-Wallis test with Dunn's multiple test correction.

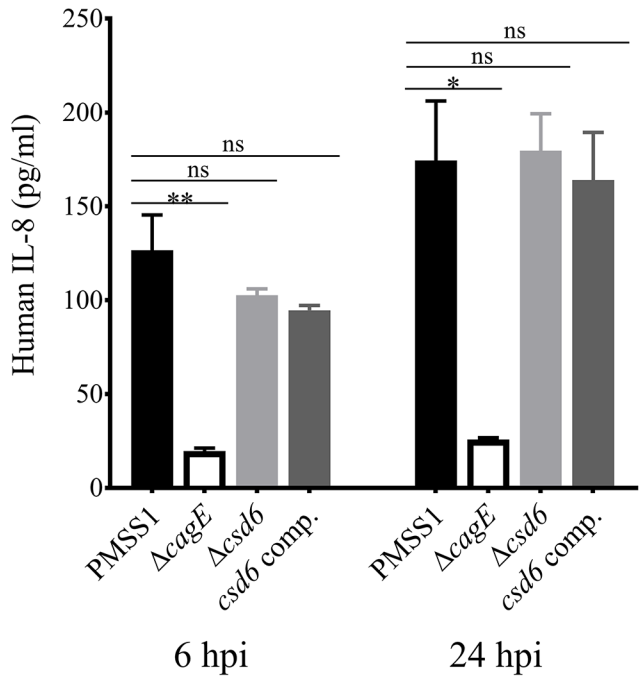

Figure S5. The Δ*csd6* mutant and *csd6* complemented strains elicit IL-8 secretion by human gastric epithelial cells. AGS cells (human gastric adenocarcinoma cell line) were infected with the wild-type PMSS1, or the PMSS1 variants Δ*cagE* (which cannot assemble the type IV secretion system), Δ*csd6*, or the *csd6* complemented strain. At the indicated time points, cell culture supernatants were harvested and IL-8 was measured by enzyme-linked immunosorbent assay. The results are shown as the mean +/- standard deviation (SD). Wild-type PMSS1 vs. Δ*cagE*, **p = 0.0097 (6 hpi) and *p = 0.0147 (24 hpi). For all other comparisons to wild-type PMSS1, no significant differences were observed (ns), unpaired t-test with Welch's correction.